Hindawi
Advances in Materials Science and Engineering
Volume 2018, Article ID 1962457, 8 pages
https://doi.org/10.1155/2018/1962457

Research Article

Performance Analysis of a Recycled Concrete Interfacial Transition Zone in a Rapid Carbonization Environment

Gongbing Yue,[1] Peng Zhang,[1] Qiuyi Li,[2] and Qianqian Li[1]

[1]*School of Civil Engineering, Qingdao University of Technology, Qingdao, Shandong 266033, China*
[2]*School of Architecture Engineering, Qingdao Agricultural University, Qingdao, Shandong 266109, China*

Correspondence should be addressed to Peng Zhang; zhp0221@163.com and Qiuyi Li; lqyyxn@163.com

Received 20 August 2017; Accepted 28 December 2017; Published 14 February 2018

Academic Editor: Charles C. Sorrell

Copyright © 2018 Gongbing Yue et al. This is an open access article distributed under the Creative Commons Attribution License, which permits unrestricted use, distribution, and reproduction in any medium, provided the original work is properly cited.

Based on the characteristics of recycled concrete interface structures, a multi-interface reconstruction model was established. To study the microstructure evolution of the interfacial transition zone (ITZ) during the carbonization process of recycled concrete, the microstructure characteristics of the ITZ of C30, C40, and C50 grade recycled concrete and the mortar matrix before and after carbonization were studied through the microhardness tester and SEM. The results show that the microhardness values of the ITZ and the mortar matrix are obviously increased and that the width of the ITZ decreases, while the ITZ performance of the C50 grade recycled concrete is not significantly changed. The ITZ exhibits a large amount of granular $CaCO_3$ after carbonization, the pores are refined, and microcracks are generated. Overall, there are significant differences in the microstructures between the ITZ and the mortar matrix before and after carbonization.

1. Introduction

With the acceleration of industrialization and urbanization, accompanied by increasing construction waste, China's annual output of construction waste has reached 3.5 billion ton, including 1.5 billion ton in the past year, which causes a significant threat to the environment in China. The resulting economic and social problems are becoming increasingly prominent [1, 2]. Recycled concrete recycles not only conserve many natural aggregate resources but also reduce construction waste pollution in the environment, in line with the requirements for the sustainable development of the construction industry. At present, scholars in various countries have conducted extensive research on the performance of recycled concrete and have found that its workability, mechanical properties, and durability are lower than those of ordinary concrete [3, 4]. Durability is the basis of engineering applications, and concrete carbonation is not only an important factor affecting concrete durability but also the main factor in the corrosion of steel [5, 6]. The carbonation reaction reduces the pH values of concrete and destroys the passivation film on the surface of steel bars, resulting in the corrosion of steel in a concrete structure.

Domestic scholars have performed systematic researches on the macroscopic properties of recycled concrete after carbonization but have conducted little researches from a microscopic viewpoint [7, 8]. Because recycled concrete is a type of multiphase, multi-interface, and heterogeneous complex alkaline material, the microstructure is more complicated than that of ordinary concrete, and the main reason for the low performance of recycled concrete is the existence of multiple weak interfacial structures [9–12]. Therefore, it is necessary to systematically study the microstructure of recycled concrete and find out the corresponding methods for improvement.

In this paper, the Vickers hardness values of the interfacial transition zone (ITZ) of recycled concrete are measured by a microhardness tester, and variations in the ITZ width and microhardness of old aggregate-old paste (LG-LJ), old slurry-new slurry (LJ-XJ), and old aggregate-new slurry (LG-XJ) interfaces are analysed, respectively. The microstructure evolution of the ITZ of the recycled concrete before and after carbonation was analysed by SEM and BES, and the mechanism of the carbonation reaction of recycled concrete was revealed.

Table 1: Basic properties of cement used in this project.

Cement type	Compressive strength (MPa)				Flexural strength (MPa)				Stability
	3 d	SD	28 d	SD	3 d	SD	28 d	SD	
P.O. 42.5	17.9	0.7	47.7	1.1	3.8	0.2	8.4	0.4	Qualified

Table 2: Technical index of coarse aggregate.

Water absorption (%)	Water content (%)	Elongated and flaky particles (%)	Crushing index (%)	Packing density (kg/m^3)	Apparent density (kg/m^3)
1.63	0.42	3.78	11.89	1449	2588

Table 3: Mixing proportion and 28-day compressive strength of the concrete samples.

Steel grade	Cement (kg/m^3)	Fine aggregate (kg/m^3)	Coarse aggregate (kg/m^3)	Water-cement ratio	28 d compressive strength (MPa)
C30	300	780	1170	0.39	39.2
C40	375	750	1125	0.35	50.7
C50	467	713	1070	0.31	61.3

2. Experiment

2.1. Raw Materials and Preparation of Test Samples. Ordinary Portland cement (P.O. 42.5) was used in this project. Table 1 lists the basic properties of cement, which were measured according to the Chinese standard [13]. Coarse aggregates were in 5 to 25 mm continuous graded limestone gravel, and the technical indicators are shown in Table 2. Fine aggregates were natural sand, and the fineness modulus is 2.5. A polycarboxylic high-performance water-reducing agent was used with a water reduction rate of 30% at an amount of 1.2%. The water used is tap water.

According to the reconstructed model of the recycled concrete multi-interface structure, core-like concrete samples (C30, C40, and C50 grades) with different strength grades were prepared, respectively. The mixing ratio of the mortar is determined by reducing the water-cement ratio by 0.02 after removing the coarse aggregate. Test concrete samples were produced with the mix ratios shown in Table 3.

Waste concrete was drilled to obtain Φ75 mm × 100 mm cylindrical core samples. The surface of the core-like concrete vertical to the size of the 100 mm cube test centre was saturated, and then different grades of cement mortar were poured (Figure 1). After the standard block was cured for 26 days, it was cut into 20 mm slices (Figure 2). Sections were divided into two groups: one group was utilized for the un-carbonated specimen and was immersed in anhydrous ethanol to terminate the hydration, and the other group underwent a rapid carbonation test based on the "Standard for Test Methods of Long-term Performance and Durability of Ordinary Concrete" (GB/T 50082-2009) [14].

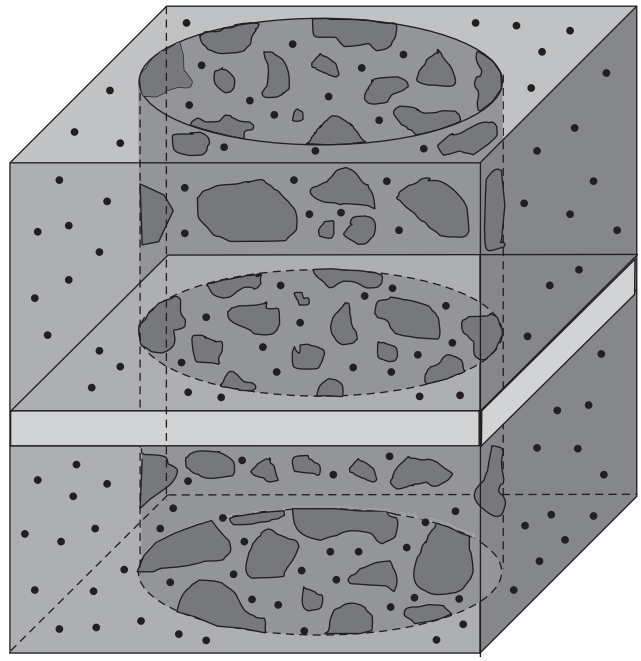

Figure 1: Waste concrete specimen with a core sample.

2.2. Test Methods and Apparatus

2.2.1. Vickers Hardness and Data Processing. The surface to be tested is prepolished as per the microhardness test requirements. As the LG-XJ and LJ-XJ interfaces exist between the interface between the core-like concrete and the new slurry, the contact surface is correspondingly similar to a straight line under a 100-fold microscope; here, in order to make it easy to identify, the beat method as the matrix point is employed. Nine indentation regions are selected, where each region is a 4×5 lattice, as shown in Figures 3(a) and 3(b). The LG-LJ interface only exists within the core-like concrete, and the appearance of aggregates causes the LG-LJ interface to appear as an irregular curve, vertical to the RBI direction. The height difference between the two adjacent sides is 10 μm, as shown in Figure 3(c).

Due to the influence of surface roughness, the fine aggregate distribution, and the unhydrated cement clinker

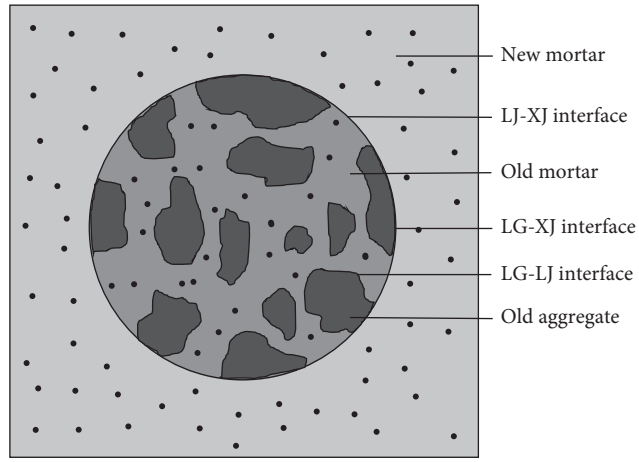

Figure 2: Section of a waste concrete specimen with a core sample.

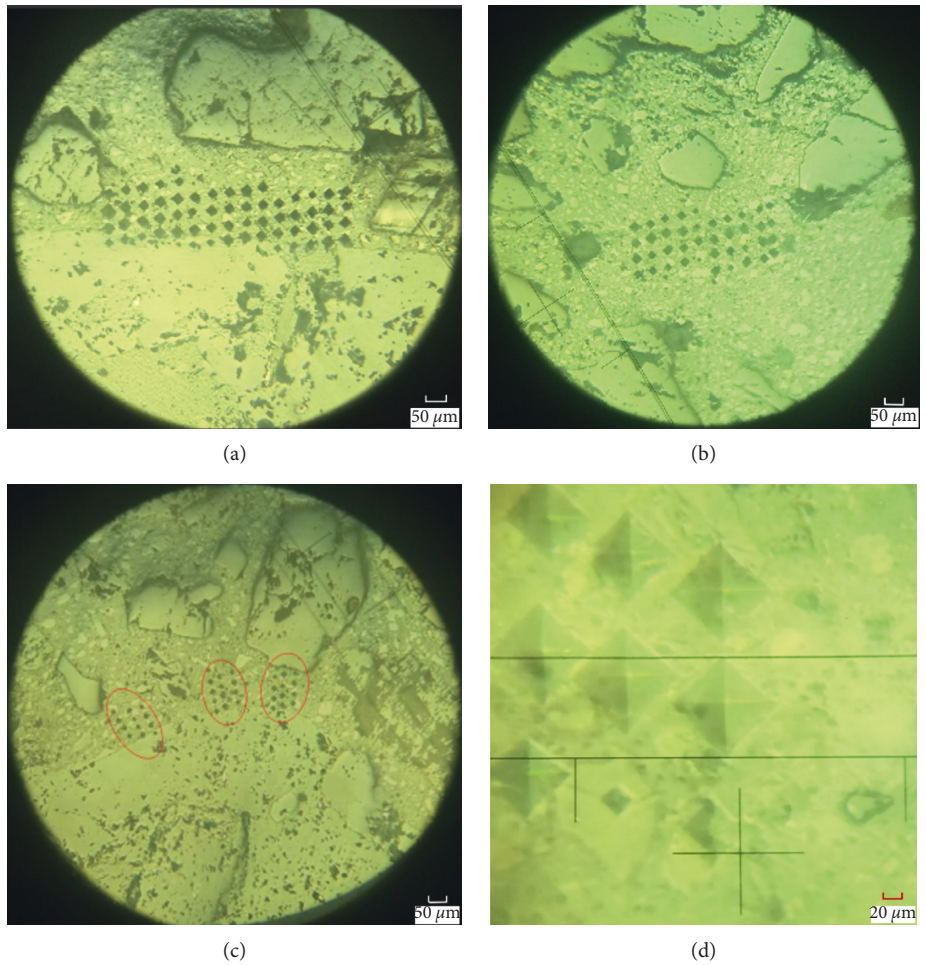

Figure 3: Three types of interface positions and RBI directions: (a) LG-XJ interface matrix point group; (b) LJ-XJ interface matrix point group; (c) LG-LJ interface vertical single-line point group; (d) the typical indent for microhardness test.

and the hole, the discrepancy in the microhardness values of the mortar matrix and the ITZ is large. Therefore, we use a box diagram to remove outliers in the RBI data, using the upper quartile and the lower quartile to determine the standard hardness of the mortar matrix standard area; thus, the width below this value is the width of the ITZ. The results for the LG-LJ interface are shown as an example in Figures 4 and 5.

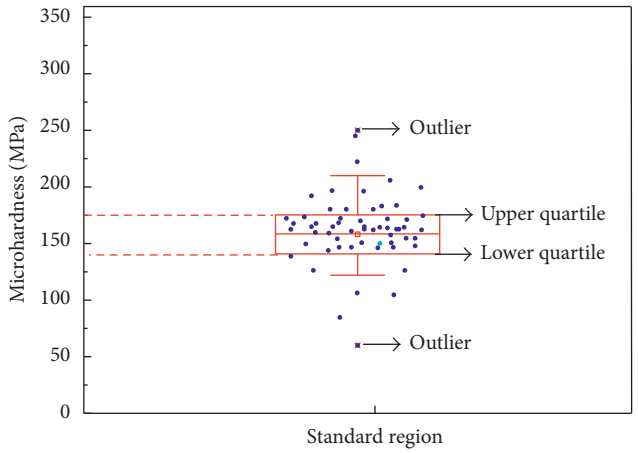

Figure 4: Schematic of the standard area box diagram method.

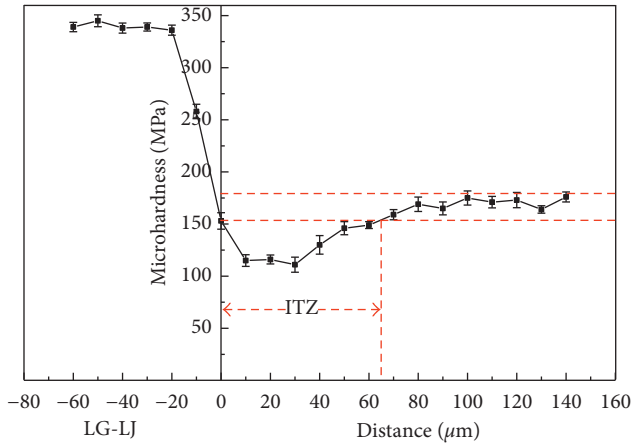

Figure 5: Interface microhardness of the LG-LJ interface.

2.2.2. Scanning Electron Microscopy. One noncarbonized sample and one sample that was carbonized for 28 days were cut into cubes of 10 mm × 10 mm × 10 mm, dried to a constant weight, and subjected to a top gold-plating treatment. The microstructure of the ITZ was observed using a scanning electron microscope (SEM, EVO18 type, Germany).

3. Results and Analysis

3.1. Microstructures of ITZ. Figures 6 and 7 show SEM images of the ITZ before and after carbonization. Based on a comparison between Figures 6(a) and 6(b), it is clear that the LG-LJ and LG-XJ interfaces are similar before carbonization. After standard curing for 28 days, the LG-XJ interface exhibits microcracks and high porosity. The interface structure is loose and filled with a large amount of CH product before carbonization. The reaction of CO_2 with CH in the weak transition zone produces $CaCO_3$, which fills some of the pores, improving the ITZ microstructure and reducing the porosity after carbonization, as depicted in Figure 7. It is noting that the H_2O produced during the reaction leaves a small hole after evaporation

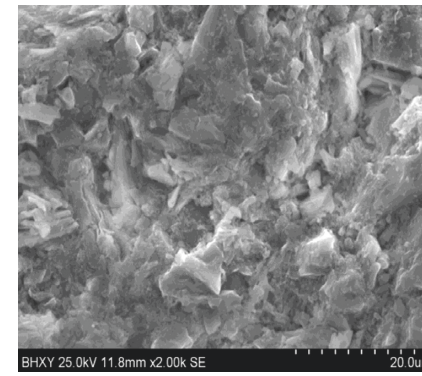

(a)

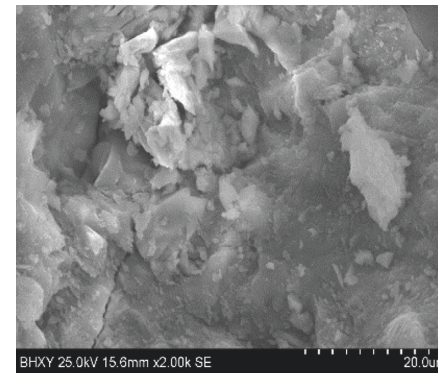

(b)

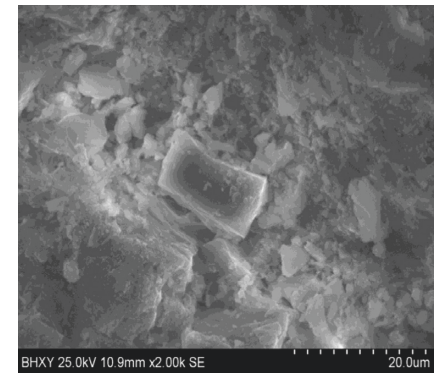

(c)

Figure 6: SEM images in different interfacial transition zones before carbonization: (a) LG-LJ interface; (b) LG-XJ interface; (c) LJ-XJ interface.

and causes the cement stone to shrink, resulting in a slight crack in the ITZ. As the hydration duration of the LG-LJ interface is long and the hydration products are rich, the interface transition area becomes denser, with less CH. Figures 7(a) and 7(b) show that carbonation effect of the latter is weaker than that of the former. As the elastic modulus and thermal expansion coefficient of the old and new mortar are similar, the micropores on the surface of the old mortar absorb the cement particles of the new mortar; thus, the new and old mortar are firmly engaged, and the ITZ is denser, which lessens the carbonization effect [15, 16].

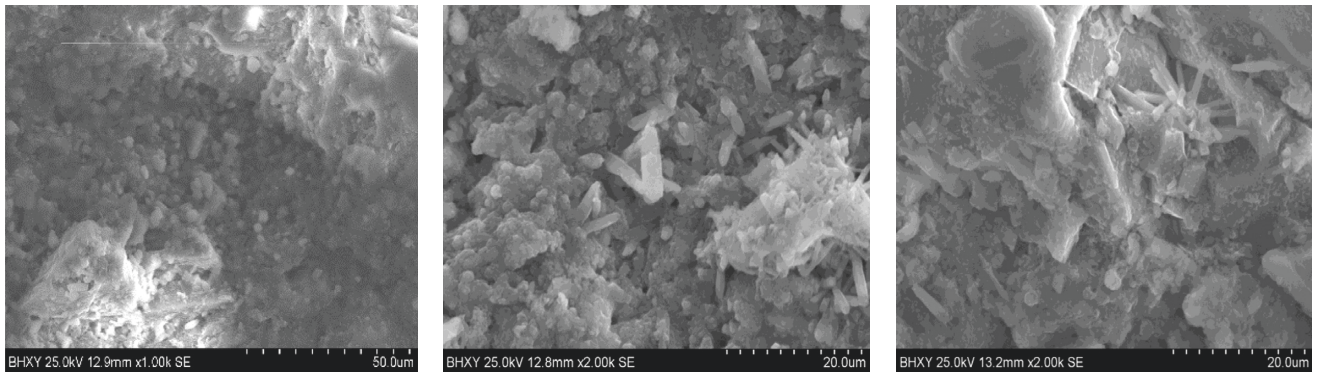

(a) (b) (c)

Figure 7: SEM images of different interfacial transition zones after carbonization: (a) LG-LJ interface; (b) LG-XJ interface; (c) LJ-XJ interface.

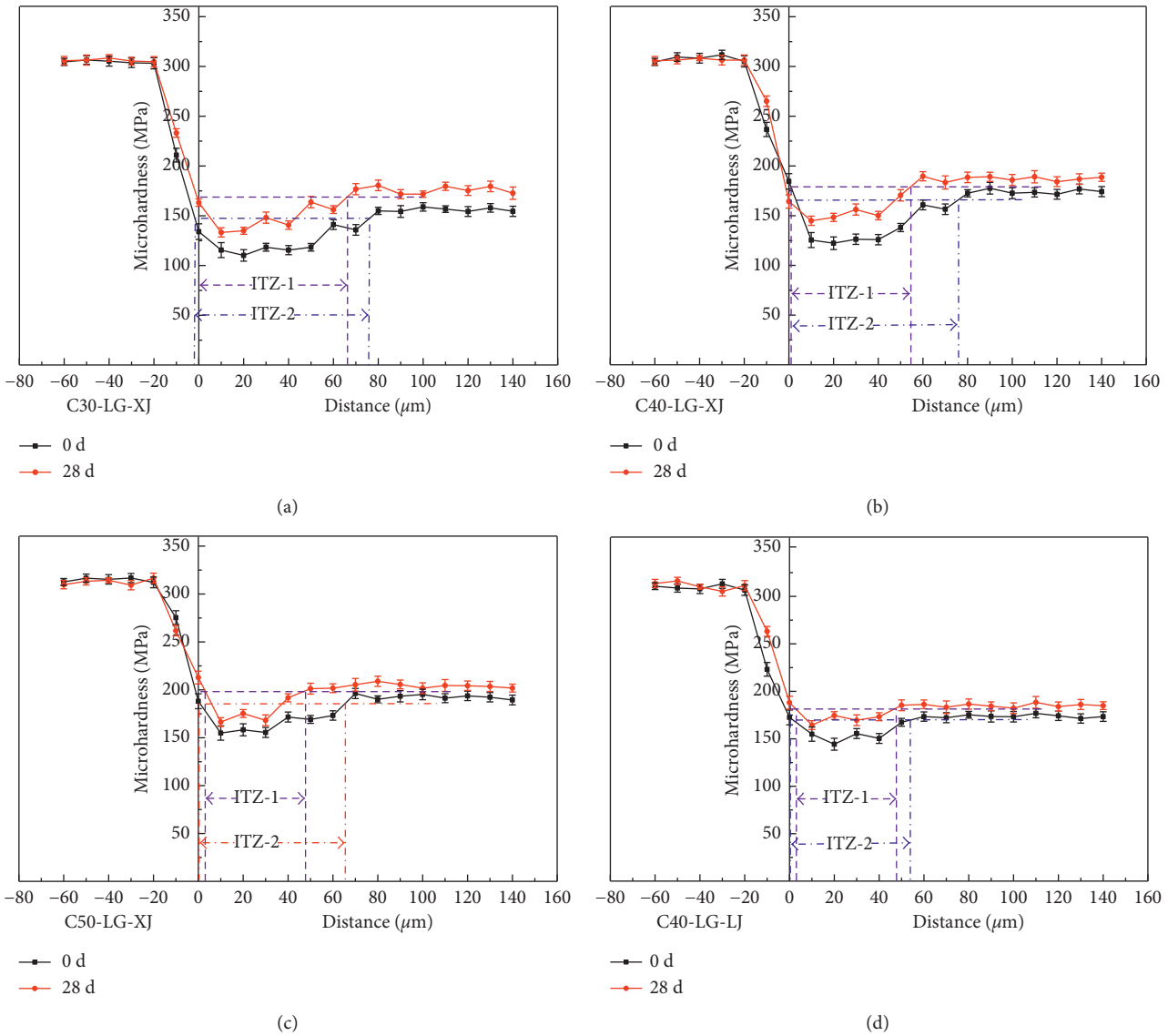

Figure 8: Effect of carbonization on the microhardness of the LG-XJ interface of recycled concrete: (a) C30 (LG-XJ); (b) C40 (LG-XJ); (c) C50 (LG-XJ); (d) C40 (LG-LJ).

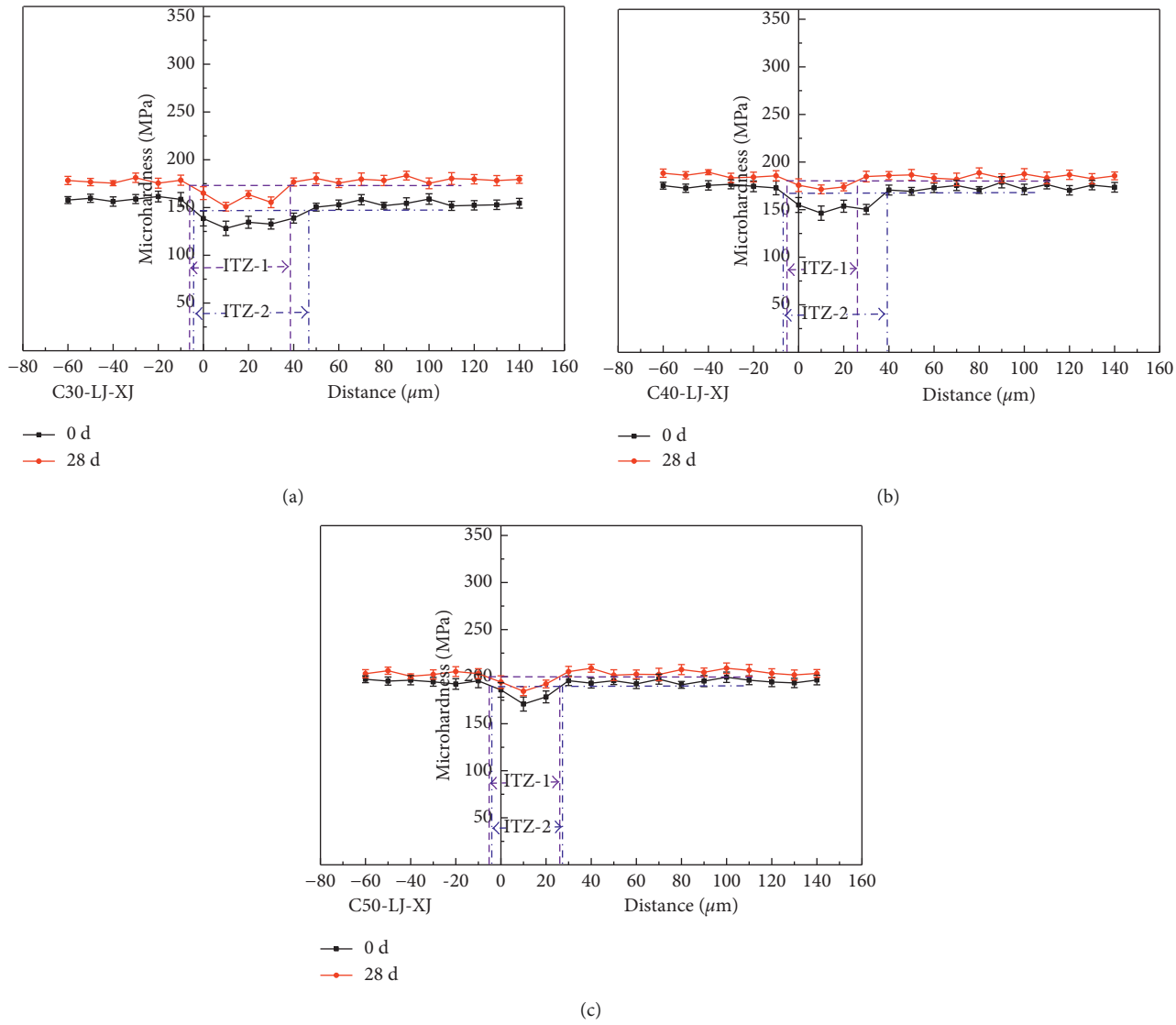

Figure 9: Effect of carbonization on the microhardness of the LJ-XJ interface of recycled concrete: (a) C30 (LJ-XJ); (b) C40 (LJ-XJ); (c) C50 (LJ-XJ).

3.2. Effect of Carbonation on Microhardness of Aggregate-Slurry Interfaces in Recycled Aggregate Concrete. In Figure 8, it can be seen that the microhardness of the LG-XJ interface increases and that the width of the ITZ decreases after 28 days carbonization; thus, the interface of low-strength-grade recycled concrete is affected by carbonization. Taking the C40 LG-XJ interface for instance, before carbonization, the ITZ microhardness is 125–171 MPa, and the ITZ width is 70–80 μm. After carbonization, the ITZ microhardness is 144–182 MPa, and the ITZ width is reduced by approximately 20 μm. Due to the sidewall effect in the LG-XJ ITZ, the porosity near the surface of the old aggregate is higher than that in the mortar matrix, which facilitates the migration of Ca^{2+}, OH^{-}, Al^{3+}, and SO_4^{2-} ions during the cement hydration process. This phenomenon leads to the enrichment of CH in the ITZ [17], and the impact of carbonation is more obvious.

Figure 8(d) shows that the difference in microhardness between the LG-LJ ITZ and the mortar matrix is relatively small, and the microhardness and ITZ width of the transition zone before and after carbonization are lower than those of the LG-XJ interface. As the C40 grade recycled concrete, the hydration duration of the LG-LJ interface is long, the cement hydration degree is high, and the zone is compact [18]; thus, the effect of carbonation on its hardness value is relatively small. The coarse aggregate itself will not be affected by the carbonation, and the microhardness value is stable.

3.3. Effect of Carbonation on the Microhardness of the LJ-XJ Interface in Recycled Concrete. Figure 9 shows that the microhardness value of the new slurry and the old slurry of the low-strength-grade recycled concrete is obviously improved. With increasing strength grade in the recycled concrete, the microhardness of the LJ-XJ interface increases, and the ITZ width decreases slightly. Taking the LJ-XJ

interface of C40 recycled concrete as an example, the microhardness values of the LJ-XJ ITZ are 170–180 MPa, and the ITZ width is approximately 40–50 μm before carbonization. After carbonization, the hardness of ITZ is 171–182 MPa, and the ITZ width is reduced by approximately 10 μm.

Compared with the LG-XJ interface, the effect of carbonation on the ITZ and mortar matrix of LJ-XJ is not obvious. As shown in the SEM image, the LJ-XJ interface is more compact, giving the ITZ a lower porosity. The moisture absorbed by the surface of the old mortar not only ensures the hydration of the cement particles around the interface but also produces a large water-filling space [19, 20]. CH cannot be fully grown in this space [21], and the microstructure of LJ-XJ ITZ can be improved, which is also an important benefit of carbonization.

4. Conclusions

(1) The carbonation reaction produces a large amount of granular $CaCO_3$, which improves the microstructure of the ITZ and reduces the porosity. Notwithstanding, the generated water vaporization can cause cracks due to cement stone shrinkage, resulting in improved pore connectivity in some sense.

(2) With the improved strength grade of the recycle concrete, the microhardness of the transitions between the LG-XJ and LJ-XJ interfaces and the new mortar matrix increases, and the width of the ITZ decreases. The transition zone of the interface with low-strength-grade recycled concrete is strongly affected by carbonization.

(3) The microhardness values of the LG-XJ ITZ and mortar matrix are increased by approximately 20 MPa. The ITZ width is reduced by 20 μm, and changes in the LG-LJ interface and LJ-XJ interface are relatively small.

Conflicts of Interest

The authors declare that there are no conflicts of interest regarding the publication of this paper.

Authors' Contributions

Gongbing Yue and Qiuyi Li conceived and designed the experiments. Gongbing Yue and Qianqian Li performed the experiments. Gongbing Yue and Peng Zhang analysed the data. Gongbing Yue and Peng Zhang wrote the paper.

Acknowledgments

Financial support of ongoing projects by the National Natural Science Foundation of China (51578297, 51378270, U1706222, and 51778309), Natural Science Foundation of Shandong Province (ZR2017ZC073 and ZR201709210171), and 111 Project is gratefully acknowledged.

References

[1] Q.-Y. Li, S. Gao, and S. Xue, *Green Concrete Technology*, China Building Materials Industry Press, Beijing, China, 2014.

[2] Z.-L. Cui and L. Chen, "Effect of recycled coarse aggregate mortar adhesion rate on the strength and drying shrinkage properties of concrete," *Bulletin of the Chinese Ceramic Society*, vol. 34, no. 2, pp. 2367–2370, 2015.

[3] V. W. Y. Tam, X.-F. Gao, and C. M. Tam, "Microstructural analysis of recycles aggregate concrete produced from two stage mixing approach," *Cement and Concrete Research*, vol. 35, no. 6, pp. 1195–1203, 2005.

[4] D.-Y. Kong, T. Lei, J.-J. Zheng et al., "Effect and mechanism of surface-coating pozzalanics materials around aggregate on properties and ITZ microstructure of recycled aggregate concrete," *Construction and Building Materials*, vol. 24, no. 5, pp. 701–708, 2010.

[5] A. Elsharief, M. D. Cohen, and J. Olek, "Influence of aggregate size, water cement ratio and age on the microstructure of the interfacial transition zone," *Cement and Concrete Research*, vol. 33, no. 11, pp. 1837–1849, 2003.

[6] M. Etxeberria, E. Vazquez, and A. mari, "Microstructure analysis of hardened recycled aggregate concrete," *Magazine of Concrete Research*, vol. 58, no. 10, pp. 683–690, 2006.

[7] C.-S. Poon, Z.-H. Shui, and L. Lam, "Effect of microstructure of ITZ on compressive strength of concrete prepared with recycled aggregates," *Construction and Building Materials*, vol. 18, no. 6, pp. 461–468, 2004.

[8] J.-Z. Xiao, Y.-D. Sun, and H. Falkner, "Seismic performance of frame structures with recycled aggregate concrete," *Engineering Structures*, vol. 28, no. 1, pp. 1–8, 2006.

[9] S.-C. Kou, C.-S. Poon, and D. Chan, "Influence of fly ash as cement replacement on the properties of recycled aggregate concrete," *Journal of Materials in Civil Engineering*, vol. 19, no. 9, pp. 709–717, 2007.

[10] W.-G. Li, M. Xiao, L. Huang, and P. S. Surendra, "Experimental study on the nano mechanical properties of the interface transition zone of recycled concrete," *Journal of Hunan University*, vol. 41, no. 12, pp. 31–39, 2014.

[11] O. Geng, R.-J. Gu, J.-J. Zheng, and B.-S. Chai, "Recycled coarse aggregate concrete interfacial microstructure development law," *Journal of Building Materials*, vol. 15, no. 3, pp. 340–344, 2012.

[12] A. K. Padmini, K. Ramamurthy, and M. S. Mathews, "Influence of parent concrete on the properties of recycled aggregate concrete," *Construction and Building Materials*, vol. 23, no. 2, pp. 829–836, 2009.

[13] GB175–2007, "Common Portland cement," 2007.

[14] GB/T 50082-2009, "Standard for test methods of long-term performance and durability of ordinary concrete," 2009.

[15] X. M. Wu, Y. Li, and Z.-F. Guan, "Tube ceramic waste regeneration of concrete and interfacial energy," *Journal of Zhengzhou University*, vol. 31, no. 2, pp. 35–38, 2010.

[16] X.-G. Wang, B.-G. Ma, and H.-B. Fu, "Interfacial mechanical properties and microstructure of gradient structure concrete," *Journal of Building Materials*, vol. 13, no. 1, pp. 101–104, 2010.

[17] J. Geng, J.-Y. Sun, L.-W. Mo, and G.-L. Zhang, "Microstructure characteristics of recycled fine aggregate and concrete," *Civil Engineering and Environmental Engineering*, vol. 35, no. 2, pp. 135–140, 2013.

[18] W.-B. Xu, Z.-H. Shui, J.-T. Ma, and W. Chen, "Study on carbonation performance of fly ash concrete based on micro hardness analysis," *Bulletin of Silicate*, vol. 30, no. 1, pp. 7–12, 2011.

[19] C.-F. Yuan, Z. Luo, T.-F. Ding et al., "Orthogonal test on carbonation behavior of recycled concrete," *Wuhan University of Technology*, vol. 32, no. 21, pp. 9–12, 2010.

[20] J.-Z. Xiao and B. Lei, "Carbonation model and structural durability design of recycled concrete," *Journal of Architecture Science and Technology*, vol. 25, no. 3, pp. 65–72, 2008.

[21] L.-F. Zhang, J.-D. Han, and W.-Q. Liu, "Research progress of microstructure evolution of cement based materials due to carbonation," *Materials Review*, vol. 29, no. 2, pp. 85–95, 2015.


The Scientific
World Journal
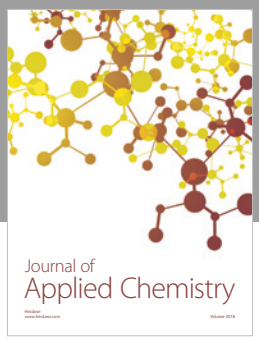
Journal of
Applied Chemistry
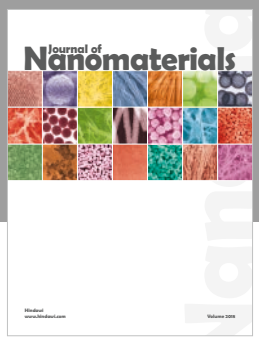
Journal of
Nanomaterials

Scientifica

International Journal of
Polymer Science
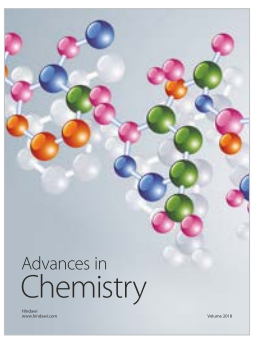
Advances in
Chemistry

Hindawi
Submit your manuscripts at
www.hindawi.com
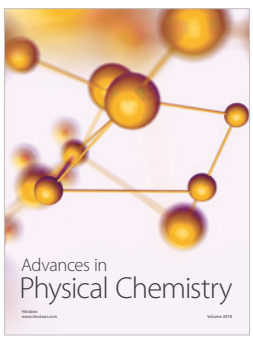
Advances in
Physical Chemistry

International Journal of
Analytical Chemistry
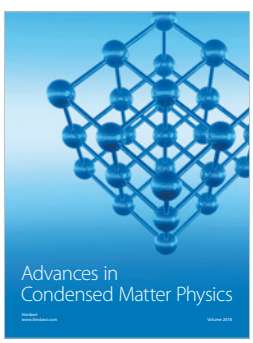
Advances in
Condensed Matter Physics
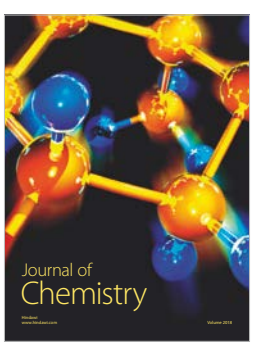
Journal of
Chemistry

International Journal of
Biomaterials
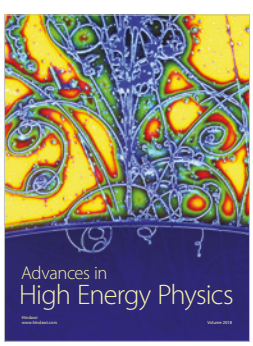
Advances in
High Energy Physics

Journal of
Engineering

Journal of
Nanotechnology

International Journal of
Corrosion

Journal of
Materials

BioMed
Research International
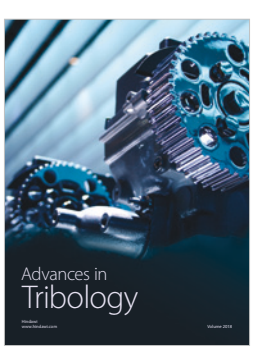
Advances in
Tribology
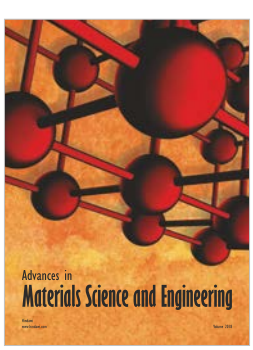
Advances in
Materials Science and Engineering